Journal of Pathology
J Pathol 2003; **199**: 368–377.
Published online 13 January 2003 in Wiley InterScience (www.interscience.wiley.com). **DOI:** 10.1002/path.1258

Original Paper

Markers for the development of early prostate cancer

Michael D Slater,[1,2] Christopher Lauer,[3] Angus Gidley-Baird[1,2] and Julian A Barden[1]*

[1] *Institute for Biomedical Research, Department of Anatomy and Histology, The University of Sydney, Sydney, NSW 2006, Australia*
[2] *Bioquest, PO Box 388, North Ryde, NSW 2113, Australia*
[3] *Missenden Medical Centre, Camperdown, NSW 2050, Australia*

**Correspondence to:*
Dr Julian A Barden, Institute for Biomedical Research, Department of Anatomy and Histology, The University of Sydney, Sydney, NSW 2006, Australia.
E-mail: julian@anatomy.usyd.edu.au

Received: 15 May 2002
Accepted: 8 August 2002

Abstract

Biochemical and genetic changes precede histologically identifiable changes accompanying cell transformation often by months or years. De-expression of the extracellular matrix adhesive glycoprotein tenascin and the cell-to-cell adherent protein E-cadherin have been suggested as markers of early neoplastic change in prostate epithelial cells. Previous studies have been inconclusive, probably due to epitope masking. This study examined 2378 biopsy cores from 289 prostates using a heat antigen retrieval protocol at low pH to improve the accuracy of detection. Tenascin and E-cadherin de-expression was correlated with purinergic receptor and telomerase-associated protein labelling, as well as prostate-specific antigen (PSA) levels and Gleason scores. E-cadherin was a poor marker, as it was expressed in all lesions except carcinomas of the highest Gleason score. Tenascin was maximally expressed in the extracellular matrix and acinar basement membrane in normal and prostatic intraepithelial neoplasia tissue. In prostate cancer tissue, tenascin expression did not correlate with Gleason score but was significantly de-expressed as purinergic receptor and telomerase-associated protein expression increased. Marked changes in tenascin, telomerase-associated protein, and purinergic receptor expression were apparent before any histological abnormalities were visible by haematoxylin and eosin (H&E) stain, making these potential markers for early and developing prostate cancer. Moreover, the potential increased accuracy of diagnosis of underlying prostate cancer using purinergic receptor translocation (PRT) assessment suggests that PSA levels may be more accurate than has generally been supposed when apparent false negatives arising from H&E-based diagnoses are correctly categorized.

Keywords: **prostate cancer; purinergic; telomerase; cell adhesion; tenascin; E-cadherin**

Introduction

To become invasive, prostate cancer cells must first penetrate histological barriers such as the acinar basement membrane proteins and extracellular matrix adhesive glycoproteins. In prostatic intraepithelial neoplasia (PIN), neoplastic acinar epithelial cells are prevented from invading the interstitium by basement membrane components such as collagen IV, laminin, fibronectin, CD44, and heparan sulphate proteoglycan (perlecan) [1]. Other proteins may also be involved in the prevention of interstitial invasion. Tenascin is an adhesive glycoprotein found in both the extracellular matrix and the acinar basement membrane. E-cadherin is another adhesion protein that surrounds each acinar epithelial cell. These proteins have been proposed as markers for the invasive process [2]. However, inconsistent results have been obtained when expression levels have been measured, possibly due to epitope masking.

The tenascin literature is ambiguous. Some workers have proposed that tenascin is involved in the maintenance of normal prostatic stromal–epithelial homeostasis [3] and protects against the effects of neoplasia. This view is supported by studies that show that tenascin is secreted by stromal cells and fibroblasts, but not by prostate cancer cells [4,5]. In this scenario, tenascin acts as a defence mechanism against the degradation of basement membrane components by neoplastic metalloproteases [6–9]. Similarly, studies have shown that patients with high tenascin expression have a better long-term survival than patients with weak or absent tenascin expression [10]. Conversely, other studies indicate that tenascin is secreted by cancer cells and that tenascin expression is required for stromal invasion [11–14]. Another study suggested that tenascin immunoreactivity does not appear to correlate with currently used prognostic indicators at all [15]. Perhaps these contradictory results reflect the inherent difficulty in reliably labelling the tenascin epitope. This may be due to the incorporation of tenascin in fibronectin matrix fibrils, under the control of heparan sulphate glycosaminoglycans and its proteoglycan core perlecan, causing masking of the epitope in both the basement membrane and the extracellular matrix [16].

Similarly, reports of E-cadherin expression in cancer have been contradictory. Cadherins are a family of glycoproteins that act as 'glue' between adjacent epithelial cells. Suggestions have been made that prostate cancer cells induce de-expression of E-cadherin, which is associated with de-differentiation, invasion, and metastasis [17,18]. The prostate carcinoma cell line PC-3N also demonstrates loss of E-cadherin [19]. Another study found consistent loss of E-cadherin expression with increasing tumour grade [20]. Conversely, other studies have shown that E-cadherin expression is increased in metastatic prostate cancer [21,22] and in invasive prostate cancer tissue [23]. In view of these contradictory reports, the use of E-cadherin as a prognostic indicator has been questioned [24,25].

Telomerase is a ribonucleoprotein enzyme that can synthesize telomeres, restoring chromosomal length after cell division and leading to cellular immortalization. It has long been associated with carcinogenesis, although the nature of this relationship is not entirely clear. In at least one study, immortalization of cells by telomerase does not appear to confer other changes associated with malignancy [26]. In fact, low levels of activity have been noted in normal lung, oral mucosa, skin, oesophagus, stomach, colorectum, pancreas, prostate, bladder, kidney, cervix, and vulva. These normal tissue samples were often taken adjacent to tumours, however [27], suggesting that there may be a 'field effect' of biochemical changes associated with transformation that is not detectable using common histological stains. The authors have described a similar field effect in prostate cancer, using the three patterns of purinergic receptor translocation (PRT) [28]. Similarly, another study found telomerase activity in prostate cores diagnosed with benign prostatic hyperplasia where a focus of established cancer existed elsewhere in the same prostate [29]. Other studies have noted telomerase activity in epithelial cell cancers, premalignant lesions, and sun-exposed skin [30]. Conversely, a study in breast cancer found that only 24 of 34 (71%) infiltrating breast carcinomas (type not stated) were positive for telomerase and that no activity was seen in adjacent tissue areas or in benign lesions [31]. The telomerase antibodies used in all of these studies were raised against a sequence in hTERT. In an effort to clarify the role of telomerase, we used an antibody raised against a novel segment of the telomerase-associated protein hTP_1.

In the present study, heat and enzymatic antigen retrieval techniques were used with a range of pH values in order to develop a protocol that enabled reliable labelling of tenascin and E-cadherin. Once the optimum protocol was established, serial sections of each block were immunolabelled for the neoplastic markers $P2X_{1-2}$ and hTP_1, as well as tenascin, E-cadherin, and the standard haematoxylin and eosin (H&E) stain. Labelling for $P2X_{1-2}$ was included because of its recent discovery as a consistently reliable marker for the initial biochemical changes indicating very early neoplastic transformation in the prostate [28].

Materials and methods

We examined 2378 cores taken from different areas of the prostates from 289 patients. We have expressed the results by case rather than core by core, as the Gleason score takes into account all the examined cores while PRT exhibits a field effect, with the same PRT pattern being seen in all the cores of the same case. A total of 23 cases were confirmed as normal; 77 as preneoplastic or very early neoplastic (by PRT assessment), including PIN; and 189 contained carcinoma. Of the Gleason-scored cancer cases, 3% were low grade (Gleason score 4 or lower), 85% were medium grade (Gleason score 5–7), and 12% were high grade (Gleason score 8–10). Tissue samples were supplied as 4–5 μm paraffin-embedded sections from prostate core biopsies on glass slides. These were dewaxed in two changes of fresh Histoclear for 10 min each and rehydrated. The sections were incubated for 5 min in 0.3% hydrogen peroxide in 1% bovine serum albumin in phosphate-buffered saline (PBS) and washed in PBS three times, 5 min per wash. Approximately serial sections from each case were labelled without antigen retrieval, as well as with enzyme and heat antigen retrieval protocols at high (10), low (2), and physiological (7) pH.

For enzymatic retrieval, the contents of one packet of pepsin (DAKO Corp, Carpinteria, CA, USA) were dissolved in 500 ml of 0.2 N HCl. This solution was preheated in Coplin jars to 37 °C in a convection oven. The deparaffinized and H_2O_2-treated slides were placed in Coplin jars for 15 min at 37 °C. They were then removed and washed in distilled water.

Heat antigen retrieval (HAR) was carried out in Target Retrieval Solution (DAKO Corp, Carpinteria, CA, USA). Solutions at pH 10.0, 7.0, and 2.0 were prepared. Slides were tested at 100 °C for 10 min, 90 °C for 30 min, 80 °C for 50 min, and 70 °C for 1 h at each pH. The slides were allowed to cool to room temperature and then washed in buffer. Thereafter, they were placed in a solution of 5% normal horse serum (0.5 ml of horse serum in 10 ml of PBS) and washed in PBS for 2 min, to block non-specific labelling.

Production of hTP_1 antiserum

The consensus sequence of human telomerase-associated protein (TP_1) [32] was examined for suitable epitopes. A segment in the C-terminal domain corresponding to the segment Cys2524–Glu2540 was chosen and the peptide synthesized using standard t-BOC chemistry on an ABI synthesizer [33]. After HPLC purification, the peptide was cross-linked to diphtheria toxin using maleimidocaproyl-*N*-hydroxysuccinimide. The peptide–antigen conjugate was suspended in

water at 5 mg/ml and aliquots were emulsified by mixing with Complete Freund's Adjuvant. Emulsion volumes of 1 ml containing 2 mg of peptide epitope were injected intramuscularly into a sheep, with second and subsequent boosts at intervals of 6 weeks using Incomplete Freund's Adjuvant. Bleeds via venepuncture were obtained after 12 weeks when adequate antibody titres had been obtained. The blood was incubated at 37 °C for 30 min and stored at 4 °C for 15 h, after which the serum was collected following centrifugation and stored at −20 °C in small aliquots. Sera were tested with an ELISA assay. The titre of the antibody used in the experiments, defined as the reciprocal of the serum dilution resulting in an absorbance of 1.0 above background in the ELISA assay, was in the range 82 000 ± 3300, compared with 225 ± 25 for pre-immune serum. Specificity of the hTP_1 antibody was demonstrated by pre-incubating tissue slides otherwise found positively stained with 10 μM of the peptide epitope for 10 min prior to the normal addition of the primary antibody. All such slides were devoid of all stain of the type shown in Figure 2B, compared with positive stain of the type shown in Figure 1C.

The sections were then labelled with either an equal amount of rabbit anti-human $P2X_1$ and $P2X_2$ or sheep anti-human TP_1, respectively, at a concentration of 1 : 100 in PBS for 30 min. Sections labelled with monoclonal anti-human tenascin (clone BC-24; Sigma, MO, USA) or monoclonal anti-E-cadherin (Zymed, San Francisco, CA, USA) were treated with HAR at 90 °C for 50 min. Slides were then washed three times in PBS for 10 min each, followed by a 30-min incubation with a 1 : 100 dilution of HRP-conjugated rabbit anti-mouse or donkey anti-rabbit secondary antibody (Dako, Carpinteria, CA, USA). All slides were then washed three times in PBS for 10 min each, visualized using a 0.05% solution of diaminobenzidine (DAB) for 10 min, washed, dried, and mounted in Entellan mounting medium (Merck). No counterstaining was used. In addition, approximately serial sections were stained with a standard H&E protocol. For practical, ethical, and legal reasons, only formalin-fixed, paraffin-embedded biopsies from previously diagnosed cases were used.

Method controls

Tissue that was previously known to stain positively for each respective antibody was used as a positive control. Negative controls for each labelling parameter were established by incubation with mouse IgG or either sheep or rabbit pre-immune serum (1 : 25 dilution) in BSA in PBS and also by omission of the primary antibodies. In each case, this procedure resulted in a complete absence of labelling. The sections were also incubated with a monoclonal antibody of the IgM isotype, which does not react with any known human protein (Silenus), as IgM aggregates may sometimes cause non-specific labelling. This procedure also resulted in no apparent labelling.

Labelling intensity quantitation

Actual levels of antigen were not quantified in this study, but rather relative differences in labelling intensity were determined using a standardized protocol. Differences in relative labelling density were measured using previously published methods [34,35]. In short, sections to be compared were labelled at the same time, using a single protocol. A Leica DC 200 digital camera using Leica 'DC Image' capture software was mounted on a Leitz Diaplan research microscope. The illumination remained fixed at 5 V. The exposure compensation option of the camera was deactivated and the resolution set at 1798 × 1438 dpi. These precautions ensured that all the images were taken under identical conditions and could therefore be validly compared. Images were saved in TIFF format, transferred to a Macintosh G4 computer, and opened without alteration directly into NIH Image 1.6 (Wayne Rasband, http://rsb.info.nih.gov/nih-image/). This resulted in an image of each acinus that occupied approximately half the field of view. Using the freehand selection tool, the prostatic epithelium component (only) of each acinus was selected and the labelling intensity of the image analysed, resulting in mean and standard deviation values. The reproducibility of epithelial tissue selection was tested by outlining a single defined area of epithelium ten times, resulting in a variation coefficient of only 1.0%. The alternative Welch t-test (two-tailed p value) was chosen for analysis of the data because it does not rely on the assumption that the sampled populations have equal standard deviations. It is more conservative than Student's t-test and results in a higher p value and a wider confidence interval. The null hypothesis was that the two population means were equal.

Results

Tenascin was abundant in the extracellular matrix and basement membrane in all normal tissue, tissue diagnosed with PIN, and in all cores showing features of PRT 1, indicating early neoplastic change [28], but was essentially absent in higher-grade cancer tissue from Gleason score 4. Detection of tenascin in the basement membrane was unsurprising since its co-localization with fibronectin fibrils has previously been reported [16] and is probably the source of the widely encountered epitope masking problems.

Routine immunoperoxidase protocols resulted in inconsistent and/or low levels of labelling for both tenascin and E-cadherin. Enzyme (pepsin) retrieval caused marked protein precipitation and unacceptable levels of damage to both the tenascin- and the E-cadherin-labelled tissue. Reproducible labelling was only possible using a heat antigen-retrieval (HAR) protocol at 90 °C for 30 min at pH 2.0. HAR at temperatures of 100 °C or above caused protein precipitation and tissue damage, although less than with the enzymatic methods. Of the time and temperature ranges

used, 90 °C for 30 min produced optimal results. HAR at pH 10.0 and pH 7.0 did not improve labelling, but HAR at pH 2.0 dramatically improved the labelling intensity of both tenascin and E-cadherin, even where no label had been noted using routine protocols. Without the use of HAR, labelling was inconsistent or absent for both proteins. Controls demonstrated that these results were due only to the combination of HAR and immunoperoxidase labelling, not to the HAR procedure itself.

In the present study, a significant reduction in tenascin expression was apparent in PRT 2 tissue and little or no tenascin labelling could be observed in PRT 3 tissue. We have previously demonstrated that P2X immunolabelling of prostate detected early neoplastic biochemical changes in apparently normal tissue [28]. This reduction in tenascin labelling did not correlate well with the Gleason score, as reduced expression was often already complete in tissue with a low Gleason score. Both tenascin and PRT labelling exhibited a field effect, in that while the H&E appearance of the tissue varied in different locations of the prostate, both purinergic receptor expression and tenascin degradation were seen throughout the tissue. Telomerase-associated protein expression (TP_1) completely mimicked that of the $P2X_{1-2}$ receptors. In contrast, E-cadherin labelling around each epithelial cell remained intact in tissue that was normal, benign prostatic hyperplasia (BPH), or showed evidence of PIN, as well as in all prostate carcinomas except those of the highest Gleason scores. An example of the PRT and TP_1 labelling is shown in Figure 1. An apparently normal core (by H&E stain, Figure 1A) is from a prostate that contained a tumour. The PRT stain (Figure 1B) of a serial section of the same core shows type 2 label (PRT 2) or cytoplasmic stain in the acinar epithelial

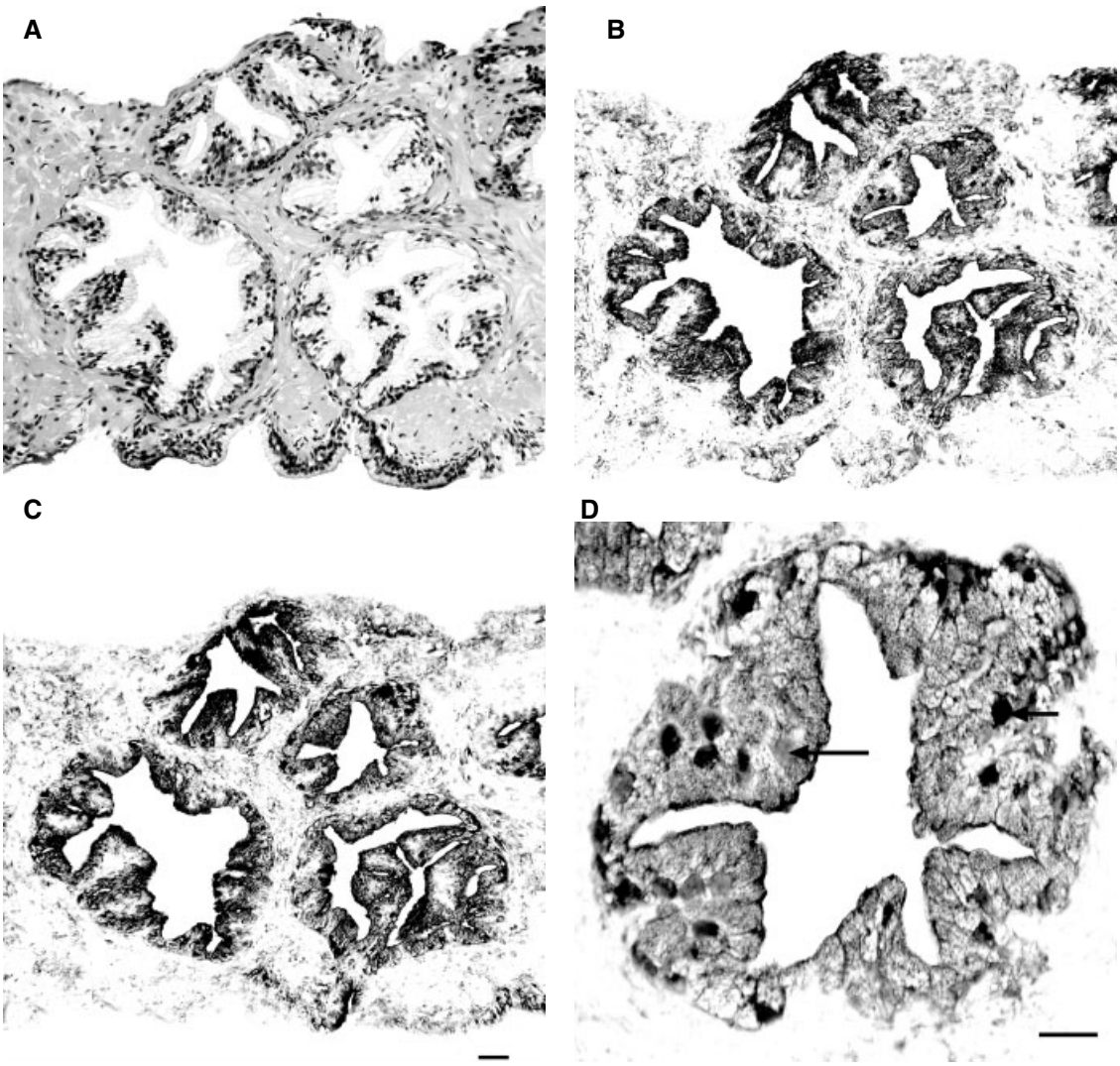

Figure 1. (A) One of three cores taken from a 47-year-old patient diagnosed as normal. In this core, no neoplastic features are evident. H&E stain. (B) The same histological area in approximate serial section, labelled with anti-$P2X_{1-2}$. The labelling features are those of PRT 2, as the anti-$P2X_{1-2}$ label is translocating through the cytoplasm. (C) The same histological area in approximate serial section, labelled with anti-telomerase-associated protein antibody. The labelling features are similar to those of the PRT label in the previous micrograph. Bar = 30 μm. (D) High-power micrograph of an acinus from the same core, labelled with anti-$P2X_{1-2}$ antibody. Note that translocating P2X puncta are visible in the cytoplasm. Some nuclei have lost their label (long arrow) and some still retain a nuclear label (short arrow). Bar = 20 μm

cells. Normal cells are completely unstained. Similarly, TP_1 label of a serial section also shows the same cytoplasmic stain (Figure 1C). A higher-power image in Figure 1D shows PRT label with several of the nuclei (short arrow) stained, but with others unstained (long arrow) as the receptors have largely moved into the cytoplasm. While BPH/normal tissue was entirely devoid of both P2X and TP_1 labelling, early cancer tissue produced labelling for both sets of markers that occurred in two well-defined patterns before the usual diagnostic histological markers of cancer became evident by H&E stain. A third pattern (PRT 3) co-localized with obvious early prostate cancer and took the form of an apical membrane deposition of the label. Overall, PRT assessment therefore involves P2X receptor expression first appearing within individual nuclei in the acini (type 1) before progressing to a cytoplasmic punctate label in the acinar epithelium, with an associated lack of nuclear stain (type 2). Finally, in advanced cases, where clear morphological evidence of cancer was apparent by H&E stain, the P2X label condensed exclusively on the apical epithelium (type 3). Of these three types of purinergic receptor translocation, PRT 1 and PRT 2 can occur in the absence of identifiable morphological change and thus appear as a field effect, whereas PRT 3 always accompanies obvious cancer by H&E stain. Reduction in tenascin expression coincided with PRT 2 and was effectively de-expressed in tissue showing PRT 3. TP_1 expression exactly matched that of P2X receptors in the present study. In both normal tissue and PIN, there was maximal expression of tenascin in the extracellular matrix and basement membrane, as well as a strong label for E-cadherin surrounding each cell. Labelling for E-cadherin was uniformly strong along the borders of each adjoining prostatic epithelial cell in normal tissue, BPH, PIN, and all grades of prostate cancer except Gleason score 8–10, where acini were no longer identifiable.

Figure 2 shows serial sections from normal prostate tissue. No prostatic hyperplasia was present by H&E stain (Figure 2A). The complete lack of label for $P2X_{1-2}$ (Figure 2B) suggests that no early neoplasia was present. Tenascin label in this tissue was strong in the extracellular matrix and acinar basement membrane (Figure 2C, arrow) and the E-cadherin label surrounding each epithelial cell was continuous and intense (Figure 2D).

Figure 3 shows an apparently normal cluster of acini (by H&E stain, Figure 3A). A core from another location in this prostate revealed the presence of prostate cancer, Gleason score 5. Some mild hyperplasia is seen (Figure 3A, arrow). The presence of translocating $P2X_{1-2}$ receptors in the cytoplasm (Figure 3B, arrow) was found in all cores, representing a field effect that suggests the presence of a tumour somewhere in this prostate. These epithelial cells are unstained in normal tissue (cf Figure 2B). Similarly, TP_1 label of a serial section also reveals the same cytoplasmic staining pattern (not shown). Figure 3C shows tenascin expression (arrows) that is only 38.4% ($p < 0.0001$) that of normal tissue (Figure 2C). This pattern was always accompanied by a PRT 2 $P2X_{1-2}$ (Figure 3B) labelling pattern and an identical telomerase label. Figure 3D shows that cell-to-cell E-cadherin labelling remains intense.

Figure 4 shows serial sections from a core biopsy from an 81-year-old man diagnosed as having Gleason score 6 prostate cancer by H&E stain (Figure 4A). The $P2X_{1-2}$ receptor label type is PRT 3, ie receptor expression condensed on the apical epithelium (Figure 4B, arrow), a labelling pattern only seen in obvious moderate–advanced cancer tissue. Figure 4C (arrow) shows that tenascin expression in the presence of PRT 3 was only 19.0% ($p < 0.0001$) that of normal tissue (Figure 2C). Despite the obvious cancer present, the E-cadherin label remained strong (Figure 4D), even though the histological architecture was itself degraded in this moderate-grade cancer tissue. These results are summarized in Table 1.

Correlation of PSA levels in each of the patients at the time of biopsy was made. A total of 23 cases were assigned normal status on the basis that there was no PRT or TP_1 label while tenascin was maximal and H&E appeared normal. The average PSA was 0.8 ± 0.1 ng/ml (mean $\pm$ SEM, range 0.1–1.8 ng/ml). Among the 77 cases found with PRT 1 and similar nuclear TP_1 label, there was no reduction in tenascin label and the H&E stain always appeared normal in all tissue cores. These early neoplastic cases showed highly elevated PSA (13.2 ± 0.8 ng/ml, range 3.0–47.8 ng/ml) compared with the established normals. The bulk of the cases numbering 189 all exhibited cancer with Gleason scores from 3 to 9. Each exhibited PRT type 2 or 3 with similar TP_1 and greatly reduced tenascin. The PSA remained essentially unchanged in this cohort from the PRT 1 cohort, with a level of 13.7 ± 0.9 ng/ml with a range of 0.5–60 ng/ml. No differences were apparent due to patient age in the cohort.

Discussion

One of the main tools of histological diagnosis is the observation of cytological and histological change as revealed by stains such as H&E. The present study adds to previous work [28] that details neoplastic biochemical changes that occur some time before the usual histological markers are visible. The P2X, TP_1, and tenascin expression patterns described were consistent throughout each core from a particular case. This field effect suggests that a biopsy does not have to sample directly the few cells that exhibit visible cancer for the presence of the tumour to be detected. E-cadherin expression was not altered by neoplasia. All normally sampled areas of an affected prostate exhibit the changes described, with PRT 1 present months to years before cancer becomes detectable by H&E stain.

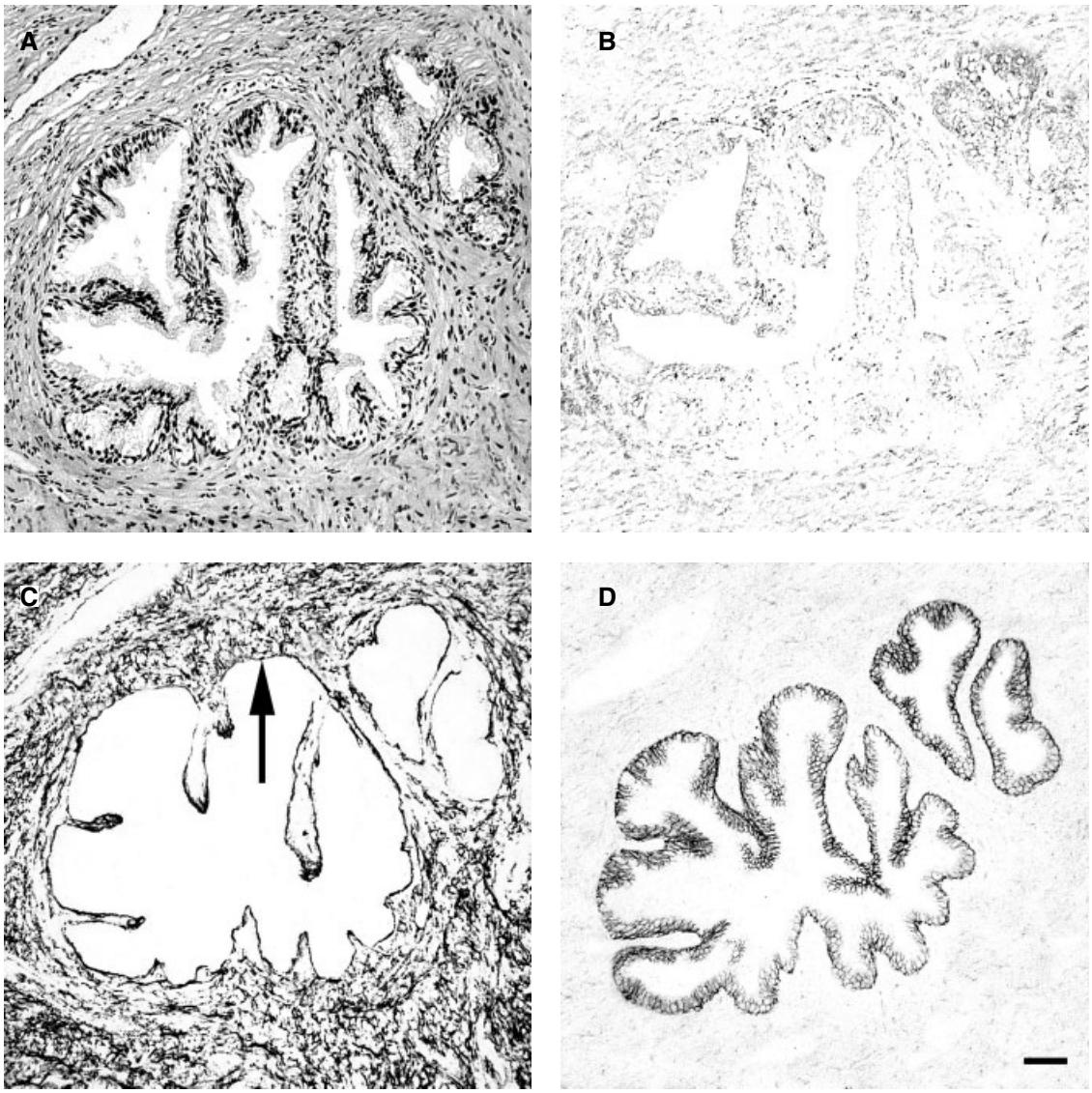

Figure 2. (A) A prostatic epithelial acinus from a 76-year-old patient. This core biopsy was originally diagnosed as being normal, with areas of benign prostatic hyperplasia (BPH). H&E stain. (B) The same acinus in approximate serial section, labelled with anti-$P2X_{1-2}$ antibody. No significant label was observed in epithelial cells, confirming the diagnosis. (C) The same acinus in approximate serial section, labelled with anti-tenascin antibody. The stroma and epithelial basement membrane are strongly labelled. (D) The same acinus in approximate serial section, labelled with anti-E-cadherin antibody. The plasma membrane of each epithelial cell is strongly labelled. Bar = 50 μm

Early markers of neoplasia are needed to improve the accuracy of diagnosis of prostate cancer. This disease is usually heterogeneous and multifocal, with diverse clinical and morphological manifestations. Current understanding of the molecular basis for this heterogeneity is limited, particularly for PIN, the only putative precursor that can be identified according to morphological criteria. It is conceivable that a stem cell of basal phenotype, or an amplifying cell, is the target of prostatic carcinogenesis. Prominent genetic heterogeneity is characteristic of both PIN and carcinoma and multiple foci of PIN arise independently within the same prostate. The strong genetic similarities between PIN and cancer strongly suggest that evolution and clonal expansion of PIN, or other precursor lesions, may account for the multifocal aetiology of carcinoma. This observation suggests that a field effect probably underlies prostatic neoplasia. This was evident in the present study. It is well known that multiple foci of cancer often arise independently, lending additional support to this hypothesis [36]. It has further been suggested that populations of secretory cells in a state of early neoplasia compound the absence of key genome protective mechanisms, thus setting the stage for an accumulation of genomic alterations and instability in high-grade PIN. This action occurs along with activation of telomerase, resulting in an immortal clone capable of developing into invasive carcinoma. Such a model predicts that genome protection remains intact in BPH, minimizing its malignant potential [37].

Apoptosis, a type of programmed cell death, is a decisive mechanism in cell processes such as homeostasis, development, and many diseases including cancer. The process of apoptosis is characterized

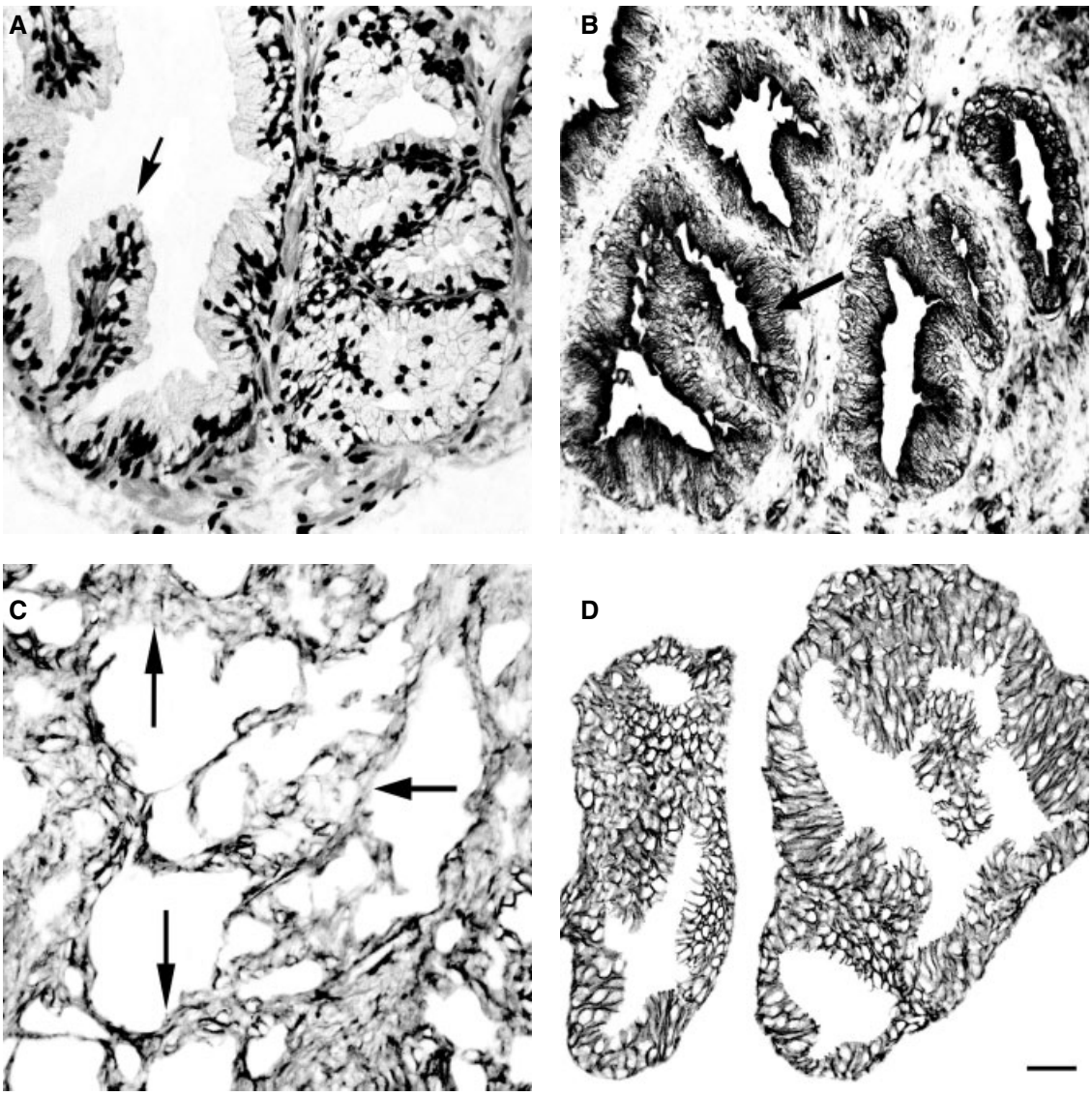

Figure 3. (A) A micrograph of a prostate biopsy core from a 57-year-old patient diagnosed as having Gleason grade 3 + 3 = score 6 carcinoma with areas of benign prostatic hyperplasia (BPH). The appearance of tissue in this particular core is normal, with some mild hyperplasia (arrow). H&E stain. (B) The same histological area in approximate serial section, labelled with anti-$P2X_{1-2}$ antibody. The features of PRT 2 (cytoplasmic puncta) are present in the acinar epithelium (arrow), indicating the presence of tumour in another area of the prostate. (C) The same histological area in approximate serial section, labelled with anti-tenascin antibody. The anti-tenascin label was only 38.4% ($p < 0.0001$) that of normal in the ECM, compared with normal tissue, and there were extensive breaks in the continuity of the basement membrane (arrows). (D) The same histological area in approximate serial section, labelled with anti-E-cadherin antibody. The appearance is that of hyperplasia. The plasma membrane of each epithelial cell is strongly labelled. Bar = 20 μm

Table 1. A total of 289 prostate cases comprising 2378 cores were examined, average age 72 ± 9 years. Each core was labelled for PRT, TP_1, H&E, tenascin, and E-cadherin

H&E, TP_1, and PRT typing	No of cases	Tenascin labelling	E-cadherin labelling
Normal by H&E PRT −ve, TP_1 − ve	23 (8%)	Maximal	Maximal
Normal by H&E PRT 1, TP_1 + ve	77 (27%)	Maximal	Maximal
Gleason score 3–4 PRT 2–3, TP_1 + ve	6 (2%)	Only 38.4% that of normal. Accompanied by PRT2	Maximal
Gleason score 5–7 PRT 2–3, TP_1 + ve	160 (55%)	Only 19.0% that of normal. Accompanied by PRT3	Maximal
Gleason score 8–10 PRT 3, TP_1 + ve	23 (8%)	8.6-fold decrease with PRT 3	Architecture degradation = antibody de-expression

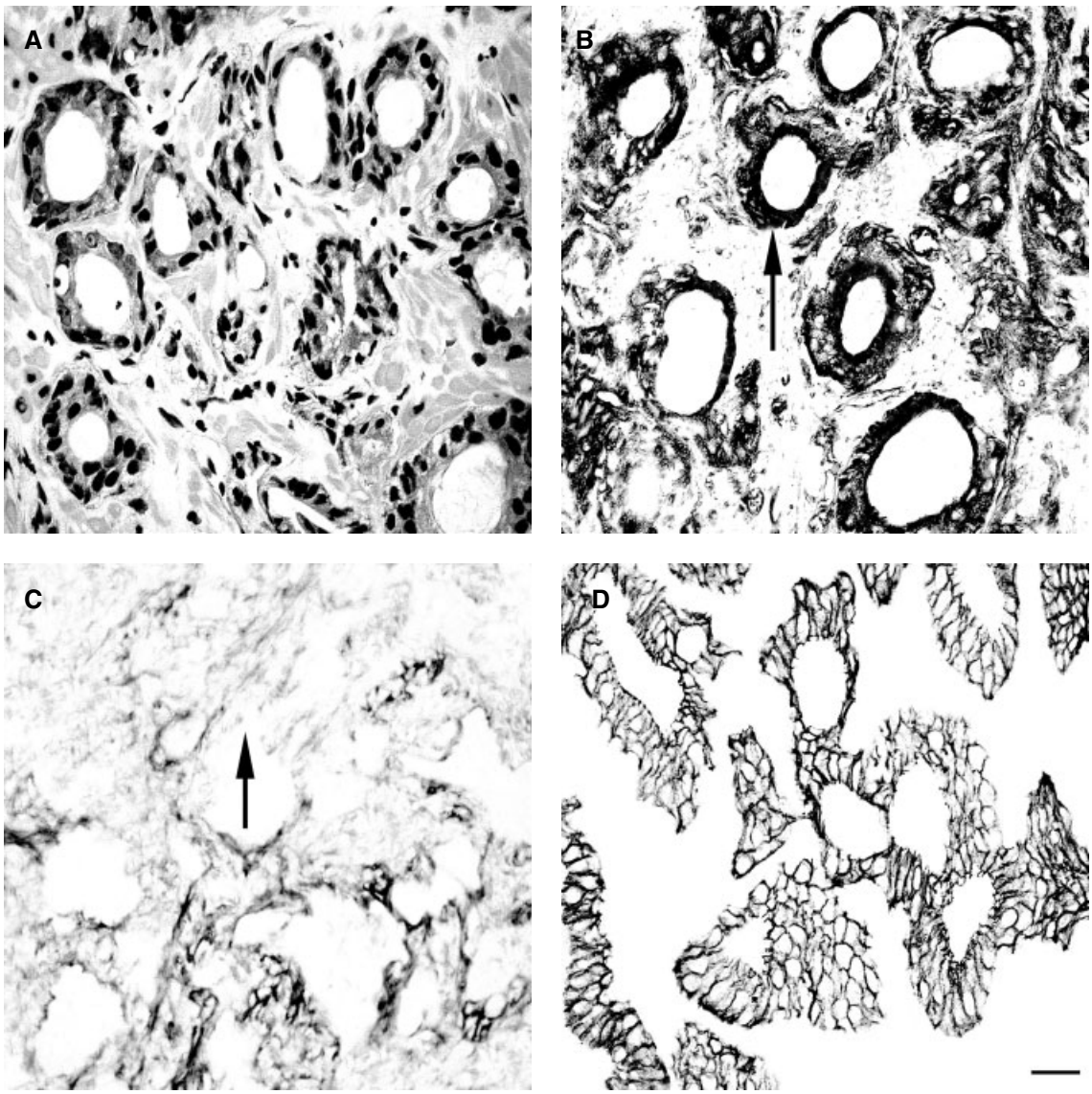

Figure 4. (A) One of three cores taken from a 61-year-old patient also diagnosed as having Gleason grade $3 + 3 =$ score 6 carcinoma. In this core, neoplastic features are evident by H&E stain. (B) The same histological area in approximate serial section, labelled with anti-P2X$_{1-2}$ antibody. The labelling features are those of PRT 3, as the anti-P2X$_{1-2}$ label is concentrated on the apical epithelium (arrow). (C) The same histological area in approximate serial section, labelled with anti-tenascin antibody. The anti-tenascin label was only 19.0% ($p < 0.0001$) that of normal in the extracellular matrix, compared with normal, and completely absent in the acinal basement membrane (arrow). (D) The same histological area in approximate serial section, labelled with anti-E-cadherin antibody. The plasma membrane of each epithelial cell is strongly labelled. Bar $= 20$ μm

by specific biochemical and morphological changes. At present, there is convincing evidence that a sustained increase in intracellular Ca^{2+} can activate cytotoxic mechanisms in various cells and tissues. Among these ionic channels, the P2X purinoreceptors and the channels of capacitative entry of calcium have been described. Pro- and anti-apoptotic molecules such as bax and bcl-2, respectively, have also been shown to participate in the process [28,38]. Direct injection of the rat prostate with an adenoviral vector that expresses Fas ligand (AdFasL/G) also results in rapid apoptosis in primary prostate epithelial cells throughout the gland [39].

Following damage to one or more of the four classes of regulatory genes — the growth-promoting proto-oncogenes, cancer-suppressor genes (anti-oncogenes), apoptosis-regulating genes, or DNA-damage repair genes, neoplastic growth may occur. This process is often accompanied by abnormalities in the expression of oncoproteins such as PDGF, FGF, EGF, CSF-1, transcriptional activators, transducing proteins, cyclins, and their receptors [40]. DNA-damage repair is crucial to prevent the proliferation of neoplastic cells. The DNA base excision repair pathway is responsible for the repair of cellular alkylation and oxidative DNA damage. A crucial step in the BER pathway involves the cleavage of baseless sites in DNA by an apurinic/apyrimidinic or baseless (AP) endonuclease (Ape1/ref-1). Ape1/ref-1 is dramatically elevated in prostate cancer. The level of staining for Ape1/ref-1 increases from low in BPH to intense in PIN and cancer, and there is an increase in the amount

of Ape1/ref-1 in the cytoplasm of PIN and cancer compared with BPH, with all tissue diagnosed by H&E stain. There was no correlation with PSA values [41]. The use of cDNA microarrays with labelled cDNA from tumour samples obtained from TURP or radical prostatectomy has identified many up-regulated transcripts. Novel prostate cancer associations for several well-characterized genes or full-length cDNAs were identified, including PLRP1, JM27, human UbcM2, dynein light intermediate chain 2, and the human homologue of rat sec61. Novel associations with high-grade PIN included breast carcinoma fatty acid synthase and cDNA DKFZp434B0335 [42]. Tissue microarray technology also promises to enhance clinical diagnosis and tissue-based molecular research greatly by allowing improved conservation of tissue resources and experimental reagents, improved internal experimental control, and increased sample numbers per experiment [43].

The present study demonstrates that $P2X_{1-2}$ and TP_1 in particular and tenascin expression to a lesser extent may prove to be reliable markers of early neoplastic transformation, while E-cadherin is unsuitable for this purpose. Moreover, the increased accuracy of diagnosis of underlying prostate cancer using the PRT typing process suggests that PSA levels are actually far more accurate than has generally been supposed when the false negatives arising from H&E-based diagnoses of sampled tissue that missed existing tumours are correctly categorized. New trials of the reagents are needed to validate further this approach.

Acknowledgement

This work was supported by the National Health & Medical Research Council of Australia.

References

1. Kammerer R, Ehret R, von Kleist S. Isolated extracellular matrix-based three-dimensional *in vitro* models to study orthotopically cancer cell infiltration and invasion. *Eur J Cancer* 1998; **34**: 1950–1957.
2. Kedeshian P, Sternlicht MD, Nguyen M, Shao ZM, Barsky SH. Humatrix, a novel myoepithelial matrical gel with unique biochemical and biological properties. *Cancer Lett* 1998; **123**: 215–226.
3. Xue Y, Li J, Latijnhouwers MA, *et al*. Expression of periglandular tenascin-C and basement membrane laminin in normal prostate, benign prostatic hyperplasia and prostate carcinoma. *Br J Urol* 1998; **81**: 844–851.
4. Pilch H, Schaffer U, Schlenger K, *et al*. Expression of tenascin in human cervical cancer — association of tenascin expression with clinicopathological parameters. *Gynecol Oncol* 1999; **73**: 415–421.
5. Doi D, Araki T, Asano G. Immunohistochemical localization of tenascin, estrogen receptor and transforming growth factor-beta 1 in human endometrial carcinoma. *Gynecol Obstet Invest* 1996; **41**: 61–66.
6. Davidson B, Goldberg I, Gotlieb WH, Ben-Baruch G, Kopolovic J. Expression of matrix proteins in uterine cervical neoplasia using immunohistochemistry. *Eur J Obstet, Gynecol, Reprod Biol* 1998; **76**: 109–114.
7. Karja V, Syrjanen K, Syrjanen S. Collagen IV and tenascin immunoreactivity as prognostic determinant in benign and malignant salivary gland tumours. *Acta Oto-Laryngol* 1995; **115**: 569–575.
8. Nerlich AG, Wiest I, Wagner E, Sauer U, Schleicher ED. Gene expression and protein deposition of major basement membrane components and TGF-beta 1 in human breast cancer. *Anticancer Res* 1997; **17**: 4443–4449.
9. Kusagawa H, Onoda K, Namikawa S, *et al*. Expression and degeneration of tenascin-C in human lung cancers. *Br J Cancer* 1998; **77**: 98–102.
10. Iskaros BF, Tanaka KE, Hu X, Kadish AS, Steinberg JJ. Morphologic pattern of tenascin as a diagnostic biomarker in colon cancer. *J Surg Oncol* 1997; **64**: 98–101.
11. Phillips GR, Krushel LA, Crossin KL. Domains of tenascin involved in glioma migration. *J Cell Sci* 1998; **111**: 1095–1104.
12. Julian J, Chiquet-Ehrismann R, Erickson HP, Carson DD. Tenascin is induced at implantation sites in the mouse uterus and interferes with epithelia cell adhesion. *Development* 1994; **120**: 661–671.
13. Yoshida T, Yoshimura E, Numata H, Sakakura Y, Sakakura T. Involvement of tenascin-C in proliferation and migration of laryngeal carcinoma cells. *Virchows Arch* 1999; **435**: 496–500.
14. Hanamura N, Yoshida T, Matsumoto E, Kawarada Y, Sakakura T. Expression of fibronectin and tenascin-C mRNA by myofibroblasts, vascular cells and epithelial cells in human colon adenomas and carcinomas. *Int J Cancer* 1997; **73**: 10–15.
15. Tokes AM, Hortovanyi E, Csordas G, *et al*. Immunohistochemical localisation of tenascin in invasive ductal carcinoma of the breast. *Anticancer Res* 1999; **19**: 175–179.
16. Chung C, Erickson H. Glycosaminoglycans modulate fibronectin matrix assembly and are essential for matrix incorporation of tenascin-C. *J Cell Sci* 1997; **110**: 1413–1419.
17. Cohen MB, Griebling TL, Ahaghotu CA, Rokhlin OW, Ross JS. Cellular adhesion molecules in urologic malignancies. *Am J Clin Pathol* 1997; **107**: 56–63.
18. Bussemakers MJ, Van Bokhoven A, Tomita K, Jansen CF, Schalken JA. Complex cadherin expression in human prostate cancer cells. *Int J Cancer* 2000; **85**: 446–450.
19. Tran NL, Nagle RB, Cress AE, Heimark RL. N-cadherin expression in human prostate carcinoma cell lines. An epithelial–mesenchymal transformation mediating adhesion with stromal cells. *Am J Pathol* 1999; **155**: 787–798.
20. Murant SJ, Handley J, Stower M, Reid N, Cussenot O, Maitland NJ. Co-ordinated changes in expression of cell adhesion molecules in prostate cancer. *Eur J Cancer* 1997; **33**: 263–271.
21. Bryden AA, Freemont AJ, Clarke NW, George NJ. Paradoxical expression of E-cadherin in prostatic bone metastases. *BJU Int* 1999; **84**: 1032–1034.
22. De Marzo AM, Knudsen B, Chan-Tack K, Epstein JI. E-cadherin expression as a marker of tumour aggressiveness in routinely processed radical prostatectomy specimens. *Urology* 1999; **53**: 707–713.
23. Kuniyasu H, Troncoso P, Johnston D, *et al*. Relative expression of type IV collagenase, E-cadherin, and vascular endothelial growth factor/vascular permeability factor in prostatectomy specimens distinguishes organ-confined from pathologically advanced prostate cancers. *Clin Cancer Res* 2000; **6**: 2295–2308.
24. Ruijter E, van de Kaa C, Aalders T, *et al*. Heterogeneous expression of E-cadherin and p53 in prostate cancer: clinical implications. BIOMED-II Markers for Prostate Cancer Study Group. *Mod Pathol* 1998; **11**: 276–281.
25. Kuczyk M, Serth J, Machtens S, *et al*. Expression of E-cadherin in primary prostate cancer: correlation with clinical features. *Br J Urol* 1998; **81**: 406–412.
26. Morales C, Holt S, Ouellette M. Absence of cancer-associated changes in human fibroblasts immortalized with telomerase. *Nature Genet* 1999; **21**: 115–118.
27. Matthews P, Jones C. Clinical implications of telomerase detection. *Histopathology* 2001; **38**: 485–498.
28. Slater M, Delprado WJ, Murphy CR, Barden JA. Detection of preneoplasia in histologically normal prostate biopsies. *Prostate Cancer Prostatic Dis* 2001; **4**: 92–96.

29. Lin Y, Uemura H, Fujinami K, *et al*. Detection of telomerase activity in prostate needle-biopsy samples. *Prostate* 1998; **36**: 121–128.
30. Ueda M, Ouhtit A, Bito T. Evidence for UV-associated activation of telomerase in human skin. *Cancer Res* 1997; **57**: 370–374.
31. Mokbel K, Parris C, Ghilchik M, Williams G, Newbold R. The association between telomerase, histological parameters, and KI-67 expression in breast cancer. *Am J Surg* 1999; **178**: 69–72.
32. Harrington L, McPhail T, Mar V, *et al*. A mammalian telomerase-associated protein. *Science* 1997; **275**: 973–977.
33. Barden JA, Cuthbertson RM, Jia-Zhen W, Moseley JM, Kemp BE. Solution structure of PTHrP(Ala15)(1–34). *J Biol Chem* 1997; **272**: 29 572–29 578.
34. Slater M. Mitochondrial DNA damage assessment using fluorescence microscopy quantitation. *J Histotechnol* 1999; **22**: 17–21.
35. Slater M, Murphy CR. Detection of apoptotic DNA damage in prostate hyperplasia using tyramide-amplified avidin-HRP. *Histochem J* 1999; **31**: 747–749.
36. Foster CS, Bostwick DG, Bonkhoff H, *et al*. Cellular and molecular pathology of prostate cancer precursors. *Scand J Urol Nephrol Suppl* 2000; **205**: 19–43.
37. De Marzo AM, Nelson WG, Meeker AK, Coffey DS. Stem cell features of benign and malignant prostate epithelial cells. *J Urol* 1998; **160**: 2381–2392.
38. Tapia-Vieyra JV, Mas-Oliva J. Apoptosis and cell death channels in prostate cancer. *Arch Med Res* 2001; **32**: 175–185.
39. Kirkman W 3rd, Chen P, Schroeder R, *et al*. Transduction and apoptosis induction in the rat prostate, using adenovirus vectors. *Hum Gene Ther* 2001; **12**: 1499–1512.
40. Cotran R, Kumar V, Collins T. *Pathological Basis of Disease* (6th edn). WB Saunders: New York, 1999.
41. Kelley MR, Cheng L, Foster R, *et al*. Elevated and altered expression of the multifunctional DNA base excision repair and redox enzyme Ape1/ref-1 in prostate cancer. *Clin Cancer Res* 2001; **7**: 824–830.
42. Bull JH, Ellison G, Patel A, *et al*. Identification of potential diagnostic markers of prostate cancer and prostatic intraepithelial neoplasia using cDNA microarray. *Br J Cancer* 2001; **84**: 1512–1519.
43. Bova GS, Parmigiani G, Epstein JI, Wheeler T, Mucci NR, Rubin MA. Web-based tissue microarray image data analysis: initial validation testing through prostate cancer Gleason grading. *Hum Pathol* 2001; **32**: 417–427.

